Final Draft
of the original manuscript:

Stark, A.; Bartels, A.; Clemens, H.; Schimansky, F.-P.:
On the Formation of Ordered Omega-phase in High Nb Containing Gamma-TiAl Based Alloys
In: Advanced Engineering Materials (2008) Wiley

DOI: 10.1002/adem.200800188

On the Formation of Ordered ω-phase in High Nb Containing γ-TiAl Based Alloys**

Andreas Stark*, Arno Bartels, Helmut Clemens, and Frank-Peter Schimansky

[*] Andreas Stark, Arno Bartels

Institute of Materials Science and Technology

Hamburg University of Technology

Eissendorfer Str. 42, D-21073 Hamburg

Helmut Clemens

Department of Physical Metallurgy and Materials Testing

Montanuniversität Leoben

Franz-Josef-Str. 18, A-8700 Leoben

Frank-Peter Schimansky

Institute of Materials Research

GKSS Research Centre

Max-Planck-Str. 1, D-21502 Geesthacht

[**] The authors gratefully acknowledge the financial support of the German Science Foundation, DFG, under the project numbers BA 1147/1-2 and GE 1115/2-2.

Abstract

The occurrence of $B8_2$ ordered ω-phase in γ-Ti-45at%Al with 5-10at% Nb during deformation as well as long-term heat-treatments was investigated. For the preparation of the alloys a powder metallurgical approach was used. The formation of ω/$B8_2$-phase was observed and analyzed by X-ray diffraction. In Ti-45at%Al-10at%Nb the β/B2-phase transforms into ω/$B8_2$-phase during cooling after hot-isostatic pressing at 1280 °C. With 5 - 7.5at% Nb the ω/$B8_2$-phase occurs during isothermal compressive deformation at temperatures around 800 °C. Here the supersaturated α_2-Ti_3Al phase after hot-isostatic pressing transforms into ω/$B8_2$-phase. Under compression stress at 800 °C the transformation is fast and needs only some minutes to take place. Without applied stress a transformation of α_2 to ω/$B8_2$-phase is also observed at 800 °C, but it takes several 100 hours. The amount of ω/$B8_2$-phase increases with increasing content of Nb. Additionally, it is shown that small carbon additions stabilize the α_2-phase and thus hamper its transformation into ω/$B8_2$-phase.

Introduction

In recent years high niobium containing γ-TiAl based alloys have been developed as structural materials in aviation gas turbines und automotive engines[1]. These so-called TNB alloys exhibit a content of 42-46at% Al and 4-10at% Nb. They have a potential of application at higher temperatures due to an improvement of high temperature strength, creep properties and oxidation resistance[2-4]. During long-term creep tests conducted on Ti-46Al-9Nb (in at%) sheets small precipitates were observed as reported in ref.[4]. By means of XRD they were analyzed as ω-phase with $B8_2$-order (short ω/$B8_2$)[5]. These precipitates occur, although the initial sheet material did not contain β/B2-phase. After long-term creep near 800 °C they occur even in massively transformed material consisting of nearly 100% γ-TiAl[5]. In general the occurrence of the ω/$B8_2$-phase is reported as a transformation of the β/B2-phase[6] and is, therefore, observed in alloys in which the high Nb content stabilizes the β-phase. For example, in Ti-40Al-10Nb the β/B2-phase transforms below 900 °C into ω/$B8_2$-phase[7]. Chen et al.[8] found the β/B2 and β/ω-phase in Ti-45Al-10Nb to be detrimental to the high temperature strength. Therefore, developers of high Nb containing TiAl-alloys should direct their attention to this microstructural instability and precipitation of ω-phase to avoid deterioration of the mechanical high temperature properties. In the present paper we describe the formation of ω/$B8_2$-phase in Ti-45Al-xNb with x = 5, 7.5, 10 at% Nb.

Experimental procedure

In order to study the influence of the niobium- and carbon content on the deformation behavior of TNB alloys compression tests were performed. The base composition was Ti-45Al with 5, 7.5 and 10Nb (in at%). One aim of this work was to determine the texture formation during compression tests. To get texture-free initial material the alloys were produced as powders in the PIGA-facility (Plasma Melting Induction Guiding Gas Atomization) at GKSS Research Centre[3]. The powder-size fraction <180µm was filled in Ti cans, degassed and subsequently hot-isostatically pressed at 200MPa for 2h and 1280 °C. The resulting fine-grained, homogenous and texture-free powder compacts are not only the perfect initial material for studying texture formation but also allow accurate Rietveld analysis of XRD patterns measured at the surface of the compacts.

The compression tests were performed on cylindrical samples (10mm in diameter and 15mm in height). The compressive strain was about ε=-1 (63% reduction in height). The tests were performed in air in the range 700 °C to 1100 °C. The strain rates were 5×10^{-2} 1/s, 5×10^{-3} 1/s, and 5×10^{-4} 1/s and thus the compression times were 20s, 200s and 2000s, followed by immediate oil quenching to avoid recrystallization effects. The specimens were cut in the center, perpendicular to the compression direction. After metallographic preparation this center plane was used for microscopy, texture measurements with XRD or for phase analysis conducted by means of a X-ray diffractometer (D8 Advance by Bruker AXS) which uses a Bragg-Brentano technique modified by a multi layer x-ray mirror to obtain nearly monochromatic Cu-K_α radiation of high density. In the case of stronger textures, i.e. after 800 °C deformation, the exact phase analysis is more complicated und a normal Rietveld analysis was not possible. All alloys were exposed to 800 °C for times up to 1000 hours and analyzed with XRD measurements. In these cases the specimens were texture free and

accurate Rietveld analysis could be performed to determine the phase compositions. The phase-models used for Rietveld refinement performed with X'Pert Plus (Philips) show an ideal stoichiometric composition, i.e. γ-TiAl, α_2-Ti_3Al and $B8_2$-Ti_4Al_3Nb, because the individual chemical composition of the phases can not be taken into account without additional information (e.g. measurements with an wavelength dispersive x-ray microprobe).

Results and discussion

Analysis after high temperature compression tests

After HIP, the Ti-45Al-10Nb shows an equiaxed microstructure with a high amount of γ-TiAl grains (gray, Figure 1a). The grains showing a bright contrast mainly consist of ω with $B8_2$ order (in the following named ω/$B8_2$) which is formed by a transformation β/B2 → ω/$B8_2$ below 913 °C[9]. Figure 1b exhibits the microstructure after deformation at 800 °C. The ω/$B8_2$ grains are flattened and show a high deformation. From texture measurements we know that this deformation causes a (001)-fiber texture of the ω/$B8_2$-phase which can only be explained by dislocation slip[10]. We can conclude that at 800 °C the ω/$B8_2$-phase does not behave brittle.

Deformation at higher temperature (1100 °C) leads also to flattened grains of the light phase in Figure 1c and it shows new small grains similar to the dynamically recrystallized grains of the surrounding γ-phase. The XRD patterns in Figure 2 identify the phase after deformation at 800 °C as ω/$B8_2$. The $B8_2$ ordering of the ω-phase can be seen only in the 100-reflection at 2Θ = 22.3° and 101 at 2Θ = 27.8° as indicated in the lower part of Figure 2 which shows calculated XRD patterns of $B8_2$-Ti_4Al_3Nb and B2-TiAl. All other reflections of $B8_2$ with significant height occur also in the disordered ω-phase. The most characteristic ω/$B8_2$-peaks occur between 39° and 40° as double peak 110 and 102. After 800 °C deformation we can assess over 10vol% ω/$B8_2$ and the very small α_2-201 peak indicates a nearly negligible amount of α_2. An exact Rietveld analysis is not possible because of the relatively strong texture after the compression test, mainly to be seen in the vanishing reflection γ-002, whereas γ-200 is strong. After deformation at 900 °C in the middle of the ω/$B8_2$ double peak a third

peak occurs. This is the 110-peak of β/B2-phase which occurs besides the ω/$B8_2$-phase. We assume the β-phase is ordered with B2 structure although we could not find the B2-100 reflection which is the indication of order. Due to the overlap with $B8_2$-101 reflection it cannot be identified in the presence of ω/$B8_2$-phase. Additionally, the B2-100 is out of reflection due to the observed B2-(111) fiber texture after compression at 1100 °C[10]. After compression at 1100 °C no specific reflections of ω/$B8_2$ can be detected and only β/B2-phase is observed.

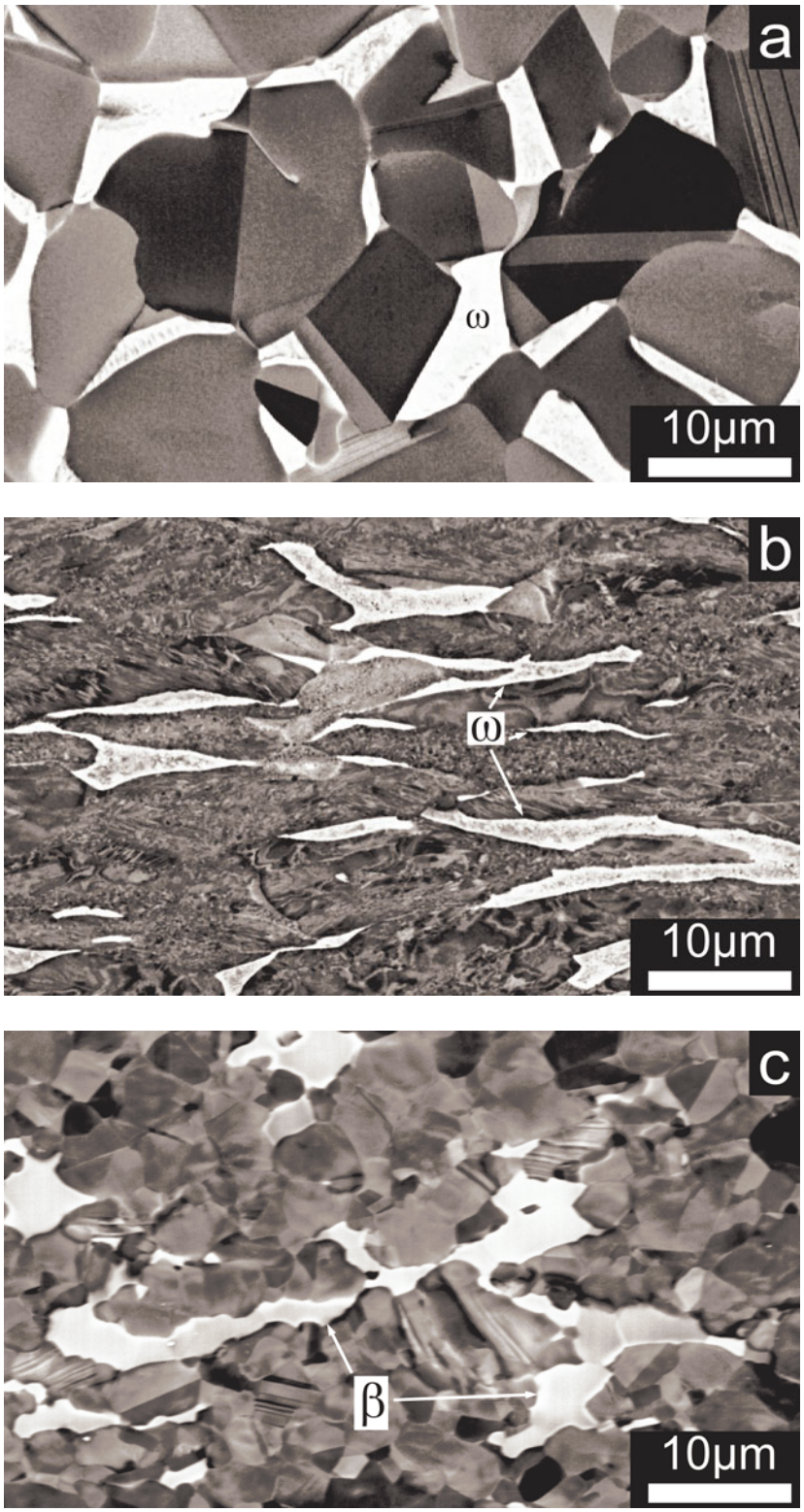

Figure 1. BSE images of the microstructure of Ti-45Al-10Nb, (a) after HIP at 1280 °C, (b) after compression test at 800 °C and (c) after compression test at 1100 °C. The ω/$B8_2$-phase and the β/B2-phase (bright contrast) are indicated by arrows.

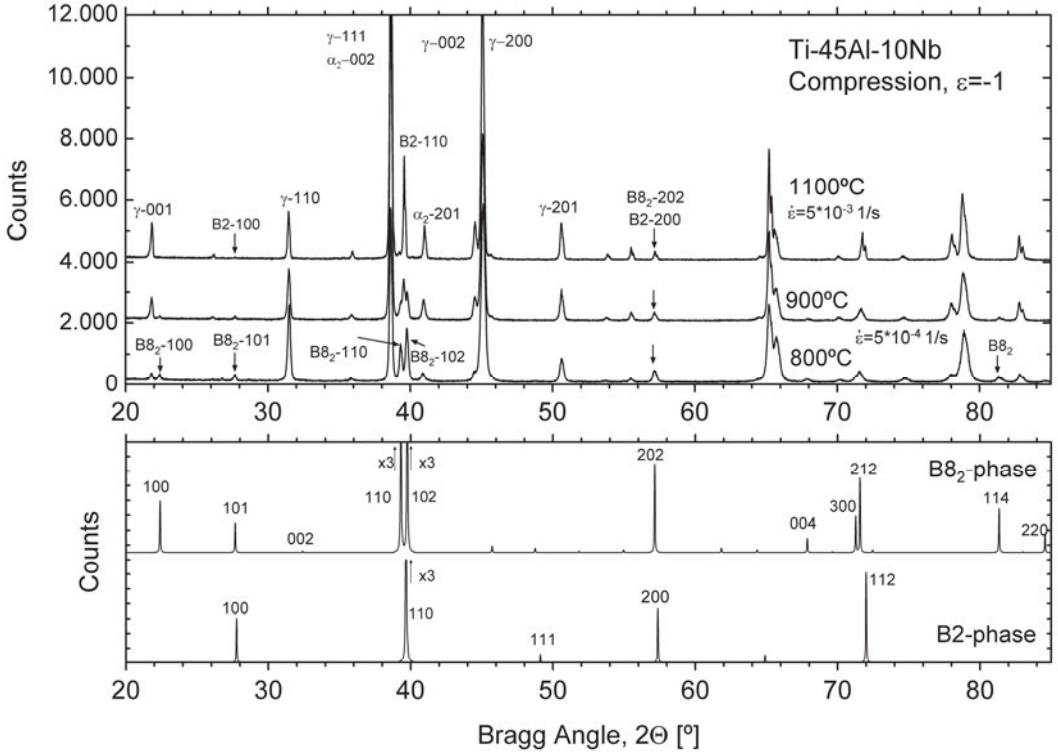

Figure 2. XRD-patterns measured with Cu-K_α radiation after compression tests. In the lower part calculated patterns of $B8_2$-Ti_4Al_3Nb and B2-TiAl are presented.

After HIP at 1280 °C there is no ω or β-phase in Ti-45Al-7.5Nb alloys. As Figure 3a demonstrates the ω/$B8_2$-phase occur during compression tests only at 800 °C and simultaneously the amount of the α_2-phase decreases. After deformation at 900 °C no ω/$B8_2$ or β/B2-phase were found. Only in the case of a compression test with duration of 2000s at 1100 °C we see a weak B2-110 reflection caused by a small amount of B2-precipitation.

The microstructure of the tested Ti-45Al-7.5Nb specimen from Figure 3a is shown in Figure 3b as BSE picture with high magnification. The deformed α_2-grains are interlaced by very fine γ-lamellae. At the grain or colony boundaries we see an extremely fine-grained structure of light and dark grains with a size of about 200nm. The grain structure is comparable with the fine grained microstructure after dynamic recrystallization in these alloys at 800 °C, but here it consists of two different phases. The very light contrasted grains are precipitations of ω/$B8_2$ and the dark grains are secondary γ which are always present in the neighborhood of the very light ω/$B8_2$-grains. The secondary γ-grains appear darker than the primary γ-grains due to a higher Al-concentration and a lower Nb-concentration. The formation of ω/$B8_2$ can be described by a reaction $\alpha_2 \rightarrow$ ω/$B8_2$ + γ. The secondary γ is necessary to accommodate the surplus Al, because the ω/$B8_2$ phase contains less Al and more Nb than α_2. Therefore, these secondary γ-grains are not only produced by spheroidization of the very thin γ-lamellae, but they also have a different composition.

The formation of ω/$B8_2$ on expenses of α_2 is also observed in Ti-45Al-5Nb which represents the alloy with the lowest content of Nb in our investigation (see Figure 3c). In comparison with Ti-45Al-7.5Nb (Figure 3a) the ω/$B8_2$-reflexes at 2Θ=39.4° and 39.7° are smaller but still visible. At the higher testing temperature of 900 °C the XRD shows also no reflexes pointing to ω/$B8_2$ or β/B2 phase.

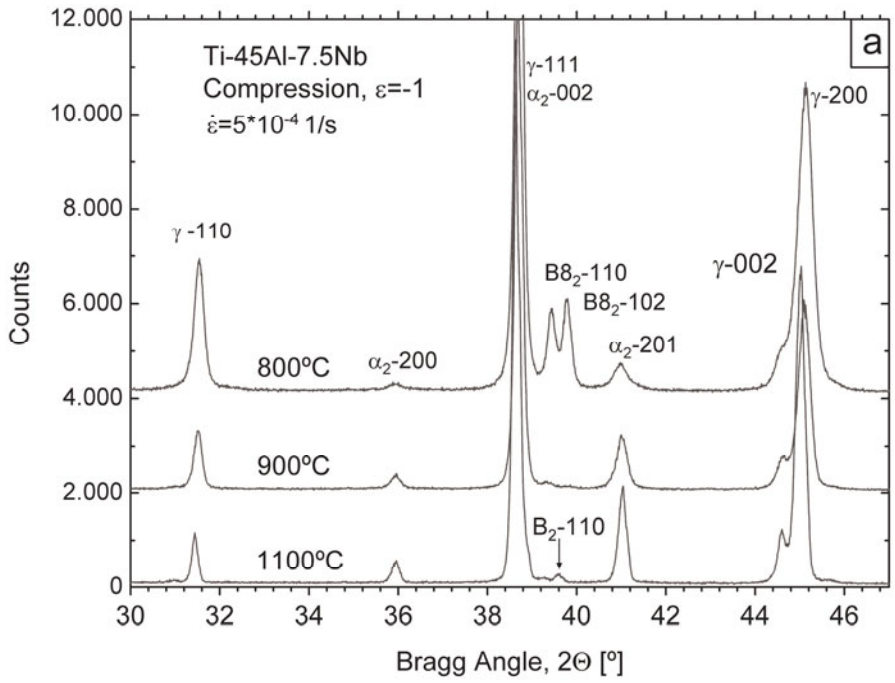
a
Ti-45Al-7.5Nb
Compression, ε=-1
ε̇=5*10-4 1/s
γ-111
α2-002
γ-200
γ -110
B82-110
B82-102
γ-002
α2-201
800ºC
α2-200
900ºC
B2-110
1100ºC
Counts
Bragg Angle, 2Θ [º]

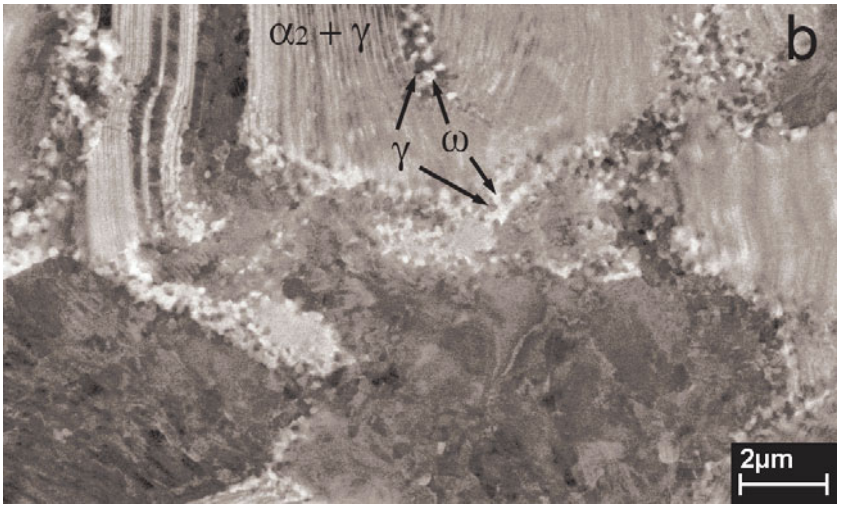
α2 + γ
b
γ
ω
2µm

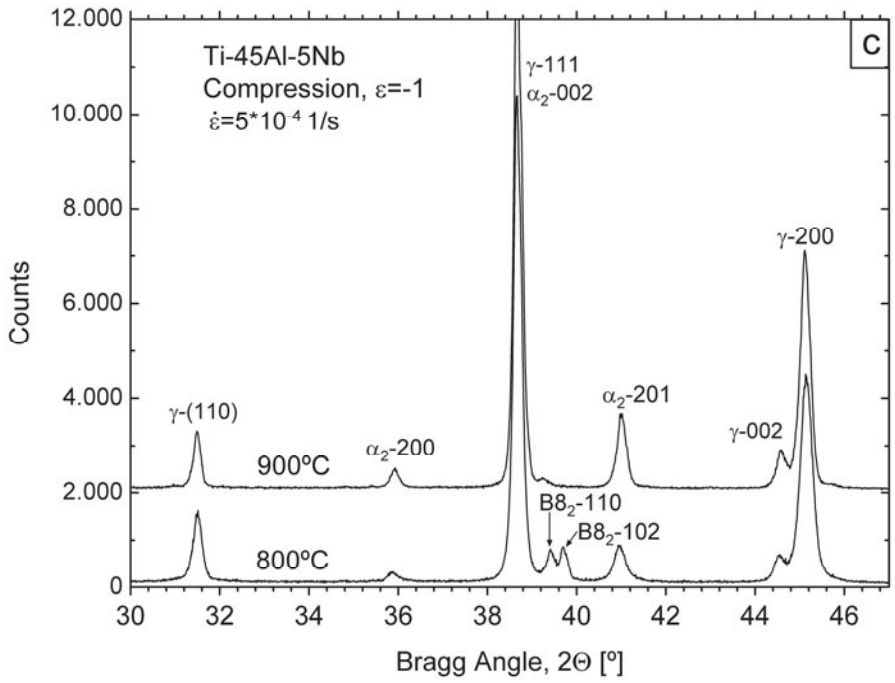

Figure 3. XRD patterns after compression tests, (a) Ti-45Al-7.5Nb tested at different temperatures. (b) Microstructure of Ti-45Al-7.5Nb after compression at 800 °C. (c) XRD patterns after compression tests conducted on Ti-45Al-5Nb.

Analysis after long-term exposure to 800 °C

Compared to the initial microstructure (Figure 4a) after a 1000 h long-term exposure to 800 °C Ti-45Al-7.5Nb shows precipitations at the grain boundaries which appear very bright in the BSE image of the microstructure (Figure 4b). With EBSD measurements (not shown in this paper) these precipitations were identified as $B8_2$ or B2-phase. The upper XRD spectrum in Figure 5a gives no indication for the existence of β/B2-phase. The strongest B2-110 reflection does not appear between the $B8_2$-110 and $B8_2$-102 reflections which are clearly separated. Obviously, the B2 and the $B8_2$ structures are so similar in the EBSD patterns, that an exact discrimination between these two phases is not possible. A similar problem is known from the tetragonal γ-TiAl structure which can be analyzed with EBSD only as fcc-structure due to the too small tetragonality. Nevertheless, the EBSD measurement gives the evidence, that the bright appearing precipitates in Figure 4b are definitely no α_2-phase and the XRD results support that they are ω/$B8_2$-phase. Their amount ob about 8 vol% in Figure 4b is nearly consistent with the 9.7 vol% estimated by Rietveld analysis. In addition, Figure 4b exhibits less α_2-lamellae than the initial state of the material in Figure 4a before the long-term exposure to 800 °C. This is a strong evidence that the formation of the ω/$B8_2$-phase happens on the expenses of the α_2-phase. In the direct neighborhood of the light precipitates (Figure 4b) we find a significant fraction of small very dark grains which are not visible in Figure 4a. They represent secondary γ-phase which contains a higher Al-concentration and probably a lower Nb-concentration than the primary γ-phase. The theoretical composition of the $B8_2$-phase is Ti_4Al_3Nb (Ti-37.5Al-12.5Nb)[6].

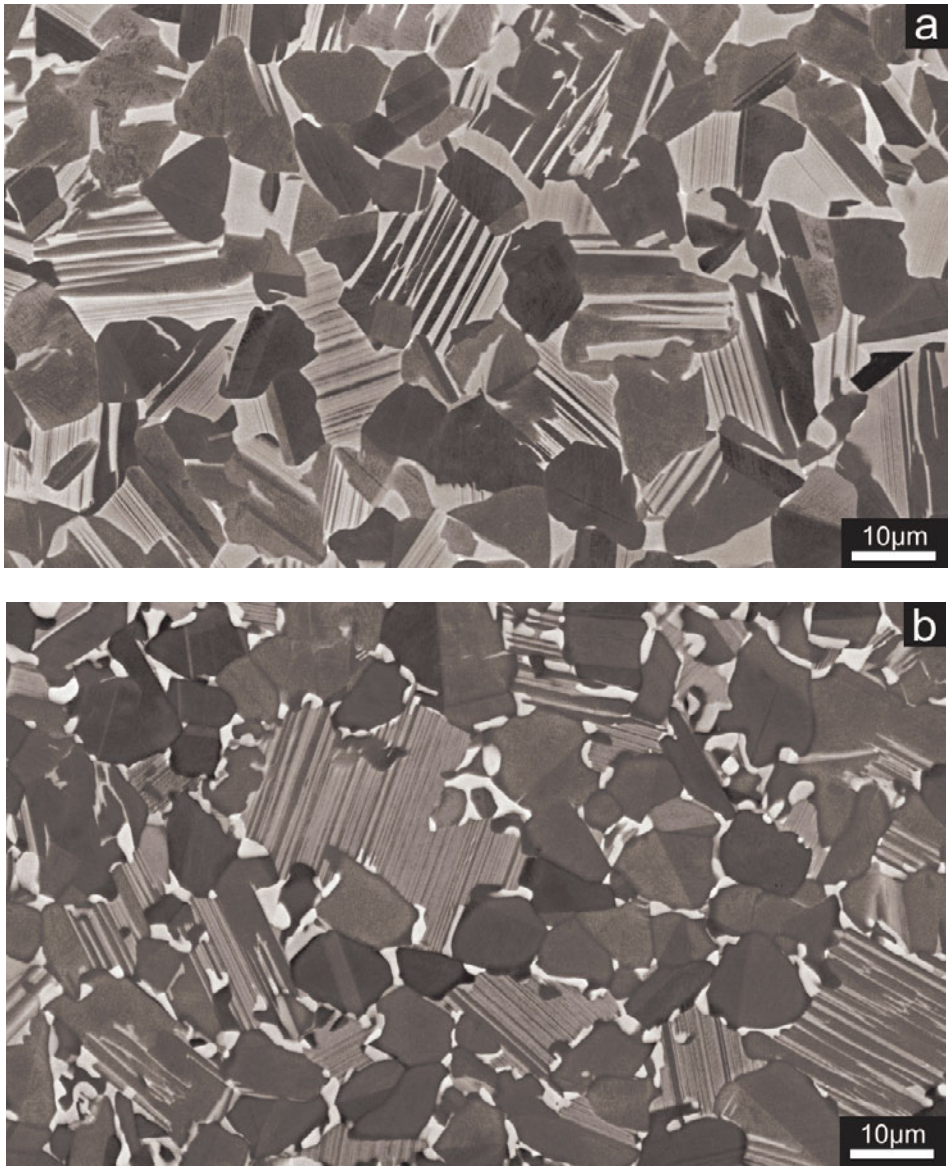

Figure 4. BSE images of the microstructure of Ti-45Al-7.5Nb, (a) initial state after HIP and (b) after 1000 h exposure to 800 °C in air.

The long-term exposure to 800 °C was applied to all three alloys Ti-45Al-(5,7.5,10)Nb in four or six isothermal annealing steps up to a total time of 1000 h. After every time step XRD measurements with a Rietveld analysis were performed. Figure 5 shows some examples of the XRD patterns. Due to well annealing conditions without internal stresses the reflections are very sharp and narrow. Therefore, we can see the splitting due to the $K_{\alpha1}$-$K_{\alpha2}$ doublet of the Cu-X ray source. Figure 5a shows the XRD patterns corresponding to the two microstructures of the initial state of Ti-45Al-7.5Nb and after exposure for 1000 h to 800 °C (Figure 4). The XRD patterns testify no dramatic change in the γ-phase, but the α_2-phase nearly vanishes and the strong $B8_2$-double reflection around 39.5° indicates the formation of ω/$B8_2$ on the behalf of α_2. The same alloy exhibits after deformation a comparable intensity of the ω/$B8_2$-reflections (Figure 3a, upper curve). But the deformation at 800 °C for 2000 s is long enough to generate a comparable amount of ω/$B8_2$-phase for which the exposure to 800 °C requires 1000 h. Thus it can be stated that the formation of the ω/$B8_2$-phase is strongly accelerated during hot-deformation. The accelerating factor of about 1800 cannot only be caused by the presence of stress but by stress-activated processes of deformation and dynamic recrystallization. The latter takes also place in the thermodynamically unstable α_2-phase and, therefore, the newly generated grains are daughter products of decomposition, i.e. ω/$B8_2$- and γ-grains. The thermal formation of ω/$B8_2$-phase takes long times because the decomposition requires long range diffusion. Due to the high content of Nb the diffusion is extremely slow at 800 °C due to a diffusion energy of about 400 kJ/mole[2,4,5].

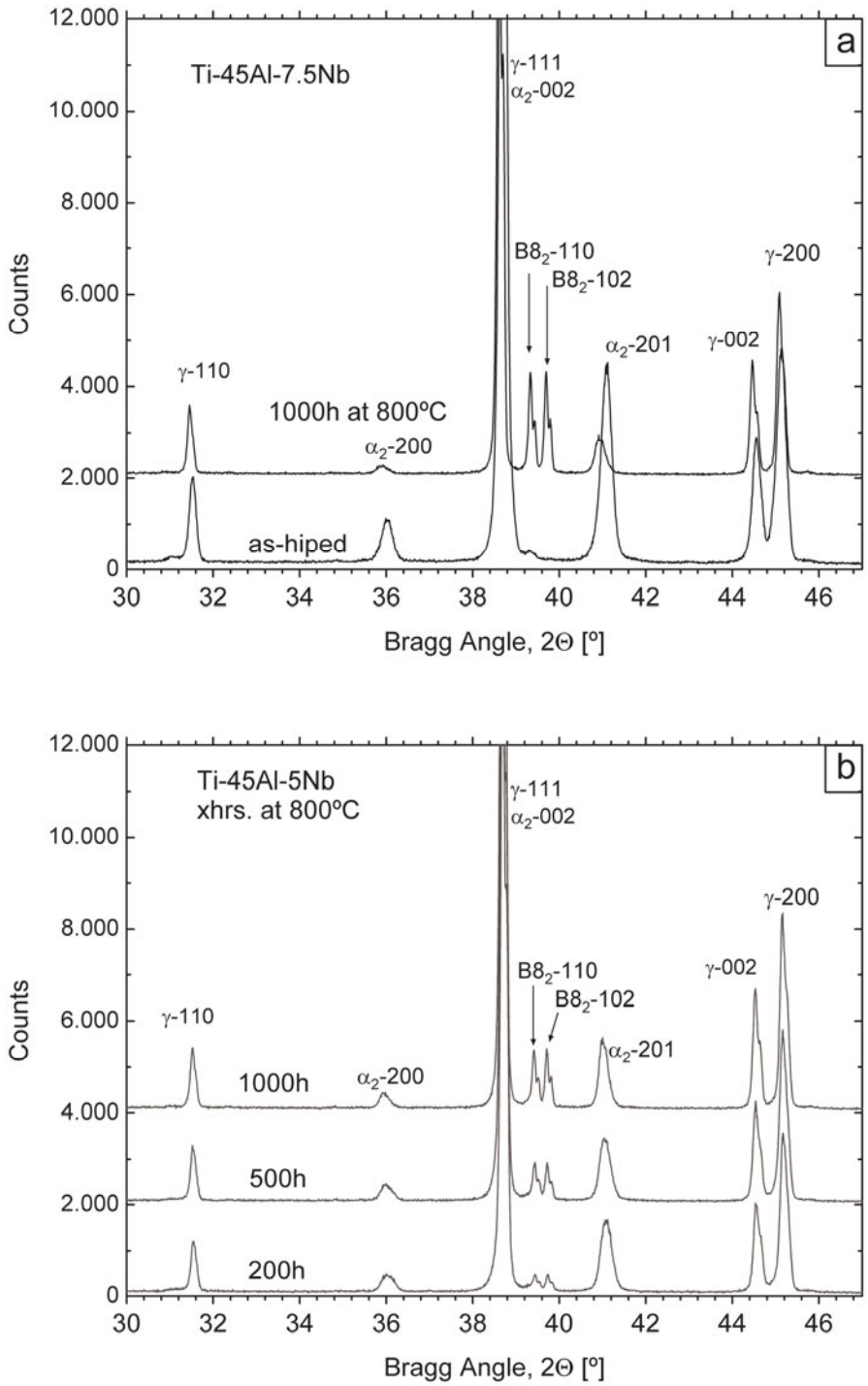

Figure 5. XRD patterns after long-term exposure to 800 °C. (a) comparison of Ti-45Al-7.5Nb in the initial state and after 1000 h exposure to 800°. (b) Ti-45Al-5Nb after different times of exposure to 800 °C.

In Figure 6 the phase contents of $B8_2$ and of α_2 as determined by Rietveld analyses are plotted versus time of exposure to 800 °C for the carbon-free Ti-45Al alloys with 5Nb, 7.5Nb and 10Nb, respectively. The supersaturation of α_2 in the as-hiped alloys decreases during the first 100 h faster than the $\omega/B8_2$-Phase increases. First the surplus α_2 transforms predominantly to γ. After longer annealing times the increase of $\omega/B8_2$ corresponds nearly to the decrease of α_2 and the content of γ-phase appears nearly constant. The question arises whether during the transformation $\alpha_2 \rightarrow \omega/B8_2$ secondary γ is formed. The initial reduction of the α_2-supersaturation is combined with a strong increase of γ-phase indicated as difference between the decreasing α_2-phase and the slowly increasing $\omega/B8_2$-phase in Figure 6. For longer times it seems to be possible that due to diffusion the existing γ in the vicinity is depleted in Nb and enriched in Al. Then only few secondary γ-phase is formed according to the Rietveld analysis which exhibits a nearly constant content of γ-phase.

Whereas we find in the initial state of Ti-45Al-5Nb and Ti-45Al-7.5Nb no $\omega/B8_2$-phase, Ti-45Al-10Nb contains initially 7.8 vol% $\omega/B8_2$-phase and only 7.4 vol% α_2 (see Table 1). No β/B2-phase can be discerned in Ti-45Al-10Nb. Also in this alloy we observe the transformation $\alpha_2 \rightarrow \omega/B8_2$. The loss of α_2 during long-term exposure to 800 °C is correlated with the increasing content of $\omega/B8_2$–phase combined with a minor increase of the γ-phase (2.0 vol%). All curves in Figure 6 give the impression that 1000 h are not yet enough time to reach definitely the thermodynamical equilibrium at 800 °C.

Table 1. Content in vol% of γ, α_2 and $B8_2$ phases in Ti-45Al-(5,7.5,10)Nb alloys as determined by Rietveld analysis using X'Pert Plus.

Ti-45Al-xNb [at%]	γ [vol%] as-hiped	γ [vol%] 1000 h at 800 °C	α_2 [vol%] as-hiped	α_2 [vol%] 1000 h at 800 °C	$B8_2$ [vol%] as-hiped	$B8_2$ [vol%] 1000 h at 800 °C
5Nb	76.4	83.1	23.6	11.3	-	5.6
7.5Nb	78.4	83.4	21.6	6.9	-	9.7
10Nb	84.7	86.4	7.4	2.8	7.8	10.8

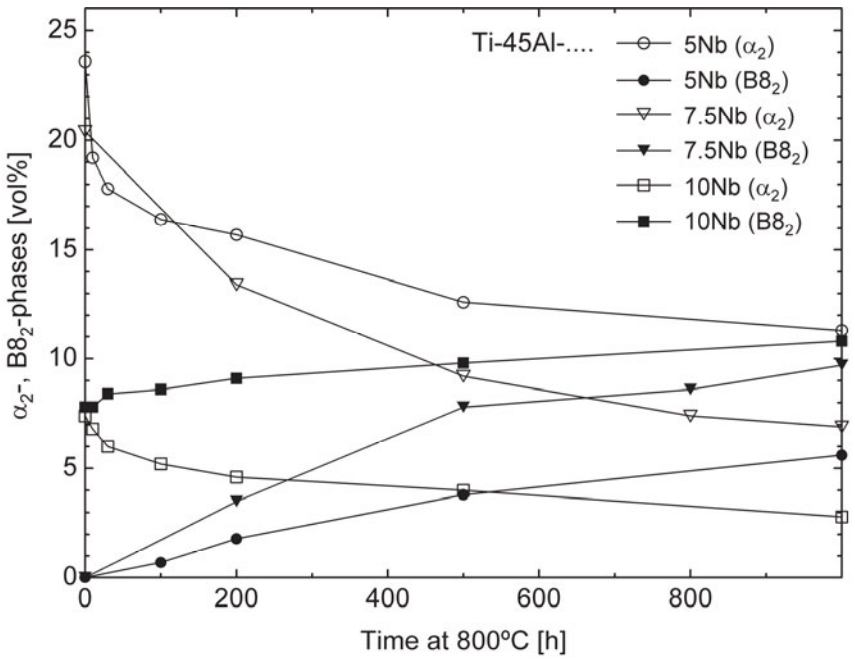

Figure 6. Phase content in vol% of $B8_2$ (closed symbols) and α_2 (open symbols) in Ti-45Al alloys with different Nb contents versus time of exposure to 800 °C as result of Rietveld analyses.

Influence of carbon additions on ω/$B8_2$-phase formation

In order to study the influence of carbon additions on the formation of the ω/$B8_2$-phase, the Ti-45Al-5Nb and Ti-45Al-7.5Nb variants were additionally alloyed with 0.25 and 0.5at% carbon. Figure 7 shows the XRD patterns of these Ti-45Al-7.5Nb+xat%C alloys after compression testing at $5x10^{-3}$ 1/s, corresponding to a relatively short test duration of 200s when, for example, compared to Figure 3a. From Figure 7 it is evident that under these test conditions the precipitation of ω/$B8_2$ is very fast in the carbon-free alloy. An addition of 0.25at% carbon significantly hampers the formation of ω/$B8_2$. A carbon addition of 0.5at% in Ti-45Al-5Nb, however, almost prevents the formation of ω/$B8_2$ and simultaneously the α_2-201 reflection is higher indicating an increased volume fraction of α_2.

In addition to compressive tests, the carbon containing alloy variants were subjected to 1000 h long-term exposure at 800 °C[11]. Also under such test conditions carbon clearly hampers the formation of ω/$B8_2$-phase. However, the suppression of the ω/$B8_2$-phase seems to be not as strong as during deformation. This gives raise to the conclusion that carbon may hinder the dynamic recrystallization during deformation[12] and, possibly, with that the formation of ω/$B8_2$-phase.

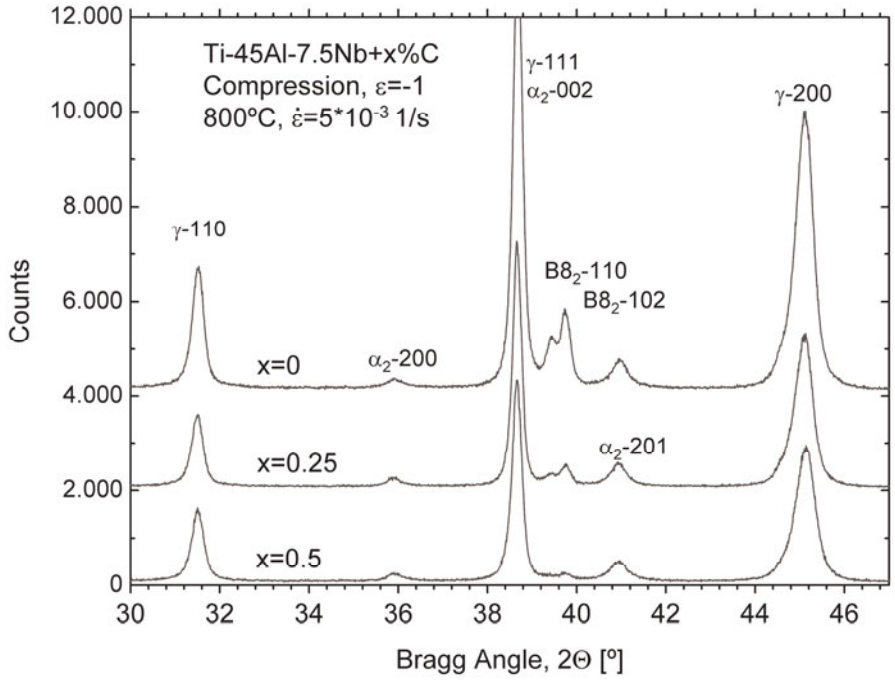

Figure 7. XRD-patterns for Ti-45Al-7.5Nb with different C-content after compression test conducted at 800 °C with a strain rate of 5×10^{-3} 1/s

Conclusions

In this study the thermal- and stress-induced formation of ordered ω/$B8_2$-phase in high Nb containing γ-TiAl based alloys have been investigated. From the obtained results the following conclusions can be drawn: At 800 °C high Nb (5-10 at%) containing alloys based on Ti-45Al show the formation of ω/$B8_2$-phase during compression testing as well as during long-term heat treatments. The amount of ω/$B8_2$-phase increases with the content of Nb (see table 1). During deformation the formation of the ω/$B8_2$-phase is completed in some hundreds seconds and is associated with the occurrence of dynamic recrystallization. Under thermal treatments the formation of ω/$B8_2$-phase is very slow and seems to be diffusion controlled. Even after 1000 h at 800 °C the equilibrium is not reached. The formation of ω/$B8_2$ is complementary to a reduction of the α_2-phase. The trans-formation $\alpha_2 \rightarrow$ ω/$B8_2$ is accompanied by the formation of new γ-phase with increased Al- and diminished Nb-content. During dynamic recrystallization new γ-grains are formed. However, during thermal treatments this new γ is generated by depletion of Nb and enrichment of Al in the neighbored grains. Therefore, the stress-induced, or better, the stress-enhanced formation of the ω/$B8_2$-phase is not only an effect of applied stress but rather a result of dynamic recrystallization under stress. Ti-45Al-10Nb contains in the initial as-hiped state 7.8 vol% ω/$B8_2$ which is a result of the transformation of the β/B2-phase during cooling below 913°C. During long-term heat treatment at 800 °C the content of ω/$B8_2$-phase increases slightly on expenses of α_2. The ω/$B8_2$-phase is deformable at 800 °C and develops a fiber-texture which is correlated by $B8_2$-(001) || B2-(111) with the fiber texture occurring above 900 °C in the β/B2-phase[11]. Therefore, we conclude that in the $B8_2$-structure dislocation slip is as easy as in the B2-structure. Consequently, the precipitation of ω/$B8_2$-phase can lead to a deterioration of the mechanical high temperature properties such as strength and creep resistance. Finally, it was

shown that small carbon additions hamper the formation of $\omega/B8_2$-phase by stabilizing the α_2-phase.

References

[1] H. Clemens, H. Kestler, *Advanced Engineering Materials* **2000,** 2, 551.

[2] F. Appel, M. Oehring, J. D. H. Paul, u. Lorenz, in *Struc. Intermetallics* TMS Warrendale, PA, USA **2001**, p.63.

[3] R. Gerling, A. Bartels, H. Clemens, H. Kestler, F.-P. Schimansky, *Intermetallics* **2004**, *12*, 275.

[4] S. Bystrzanowski, A. Bartels, H. Clemens, R. Gerling, F.-P. Schimansky, G. Dehm, H. Kestler, *Intermetallics* **2005**, *13*, 515.

[5] S. Bystrzanowski, A. Bartels, H. Clemens, R. Gerling, F.-P. Schimansky, G. Dehm, in *Integrative and Interdisciplinary Aspects of Intermetallic* MRS Warrendale, PA, **2005**, Vol. *842*, p.121.

[6] L. A. Bendersky, W. J. Boettinger, B. P. Burton, F. S. Biancaniello, *Acta metall. mater.* **1990**, *38*, 931.

[7] T. H. Yu, C. H. Koo, *Mater. Sci. Eng.* **1997**, *A239-240*, 694.

[8] G. L. Chen, W. J. Zhang, Z. C. Liu, S. J. Li, in *Gamma Titanium Aluminides* TMS Warrendale, PA, USA **1999**, p.371.

[9] H. F. Chladil, H. Clemens, G. A. Zickler, M. Takeyama, E. Kozeschnik, A. Bartels, T. Buslaps, R. Gerling, S. Kremmer, L. A. Yeoh, K.-D. Liss, *Int. J. Mat. Res.* **2007,** *98* 1131.

[10] A. Stark, A. Bartels, F.-P. Schimansky, H. Clemens, in *Advanced Intermetallic-Based Alloys* MRS Warrendale, PA, USA **2007,** *Vol. 980*, p.359.

[11] A. Stark, A. Bartels, F.-P. Schimansky, R. Gerling, H. Clemens, in *Ti-2007 Science and Technology* The Japan Institute of Metals **2007**, p.685.

[12] A Stark, A. Bartels, F.-P. Schimansky, R. Gerling, H. Clemens, in *Structural Aluminides for Elevated Temperature Applications* TMS Warrendale, PA, USA **2008**, in press

For the Table of content:

In Ti-45Al-10Nb the β/B2-phase transforms below 924 °C into $B8_2$ ordered ω-phase. During deformation of Ti-45Al-(5-7.5)Nb at 800 °C the ω/$B8_2$-phase occurs in absence of β/B2-phase on the expenses of α_2-Ti_3Al phase. During long term exposure to 800 °C a very slow transformation α_2 into ω/$B8_2$- and γ-phase is observed. Small carbon additions hamper the formation of ω/$B8_2$-phase.